

Latent Diffusion Model Based Denoising Receiver for 6G Semantic Communication: From Stochastic Differential Theory to Application

Xiucheng Wang, *Graduate Student Member, IEEE*, Honggang Jia, *Graduate Student Member, IEEE*, Nan Cheng, *Senior Member, IEEE*, Dusit Niyato, *Fellow, IEEE*,

Abstract—In this paper, a novel semantic communication framework empowered by generative artificial intelligence (GAI) is proposed, specifically leveraging the capabilities of diffusion models (DMs). A rigorous theoretical foundation is established based on stochastic differential equations (SDEs), which elucidates the denoising properties of DMs in mitigating additive white Gaussian noise (AWGN) in latent semantic representations. Crucially, a closed-form analytical relationship between the signal-to-noise ratio (SNR) and the denoising timestep is derived, enabling the optimal selection of diffusion parameters for any given channel condition. To address the distribution mismatch between the received signal and the DM's training data, a mathematically principled scaling mechanism is introduced, ensuring robust performance across a wide range of SNRs without requiring model fine-tuning. Built upon this theoretical insight, we develop a latent diffusion model (LDM)-based semantic transceiver, wherein a variational autoencoder (VAE) is employed for efficient semantic compression, and a pretrained DM serves as a universal denoiser. Notably, the proposed architecture is fully training-free at inference time, offering high modularity and compatibility with large-scale pretrained LDMs. This design inherently supports zero-shot generalization and mitigates the challenges posed by out-of-distribution inputs. Extensive experimental evaluations demonstrate that the proposed framework significantly outperforms conventional neural-network-based semantic communication baselines, particularly under low SNR conditions and distributional shifts, thereby establishing a promising direction for GAI-driven robust semantic transmission in future 6G systems.

Index Terms—Semantic communication, generative artificial intelligence, diffusion model, stochastic differential equations, noise erasing.

I. INTRODUCTION

The advent of sixth-generation (6G) wireless communication marks a fundamental paradigm shift from conventional bit-level transmission toward semantic-level information exchange [1]. Different from traditional systems that aim to faithfully reconstruct raw data at the receiver, semantic communication seeks to extract, compress, and transmit the underlying meaning of the data to fulfill the intent of the communication task

[2]. This shift is primarily driven by the growing demand for intelligent, efficient, and context-aware communication in emerging application scenarios. For instance, in extended reality (XR), the perceived user experience depends more on the accurate reconstruction of spatial semantics than on the pixel-wise fidelity of data [3]. In industrial Internet of Things (IIoT) environments, vast amounts of sensor data are generated continuously, yet only a small fraction of this data holds decision-critical value [4]. Similarly, digital twin systems require real-time synchronization between physical entities and their virtual counterparts, necessitating communication mechanisms that are capable of semantic abstraction and selective information delivery [5]. However, current wireless communication architectures, predominantly based on Shannon's information theory, are designed to ensure the reliable delivery of symbol sequences rather than understanding their semantic content. While effective in maximizing data throughput under bandwidth constraints, these systems are inherently incapable of reasoning about the contextual importance or task relevance of transmitted information [6]. As spectrum resources become increasingly scarce and the volume of data continues to grow, the limitations of bit-centric models become more pronounced. Consequently, both academia and industry are actively exploring new frameworks for semantic communication that can overcome these fundamental bottlenecks. By rethinking the role of the transmitter and receiver as semantic encoders and decoders, future communication systems must go beyond the Shannon limit and prioritize the transmission of meaningful content over syntactic accuracy [7].

Recent advances in deep learning have led to the proliferation of neural network-based semantic communication frameworks, where the end-to-end system is typically implemented as an autoencoder architecture comprising a neural encoder, a noisy channel, and a neural decoder [8]. These systems demonstrate impressive performance in compressing and reconstructing semantic features, enabling tasks such as image transmission with drastically reduced bit rates. However, despite the promising capabilities of neural network-based semantic communication systems, they exhibit significant limitations in terms of robustness and generalization. One of the most critical challenges arises from their acute sensitivity to signal-to-noise ratio (SNR) variation [9]. Specifically, the semantic features produced by the encoder are susceptible to corruption by additive noise introduced by the wireless channel, resulting in received representations at the decoder that diverge markedly

This work was supported by the National Key Research and Development Program of China (2024YFB907500).

Xiucheng Wang, Honggang Jia, and Nan Cheng are with the State Key Laboratory of ISN and School of Telecommunications Engineering, Xidian University, Xi'an 710071, China (e-mail: {xcwang_1, jiahg}@stu.xidian.edu.cn; dr.nan.cheng@ieee.org); (*Corresponding author: Nan Cheng.*)

Dusit Niyato is with the School of Computer Science and Engineering, Nanyang Technological University, Singapore. (e-mail: dniyato@ntu.edu.sg)

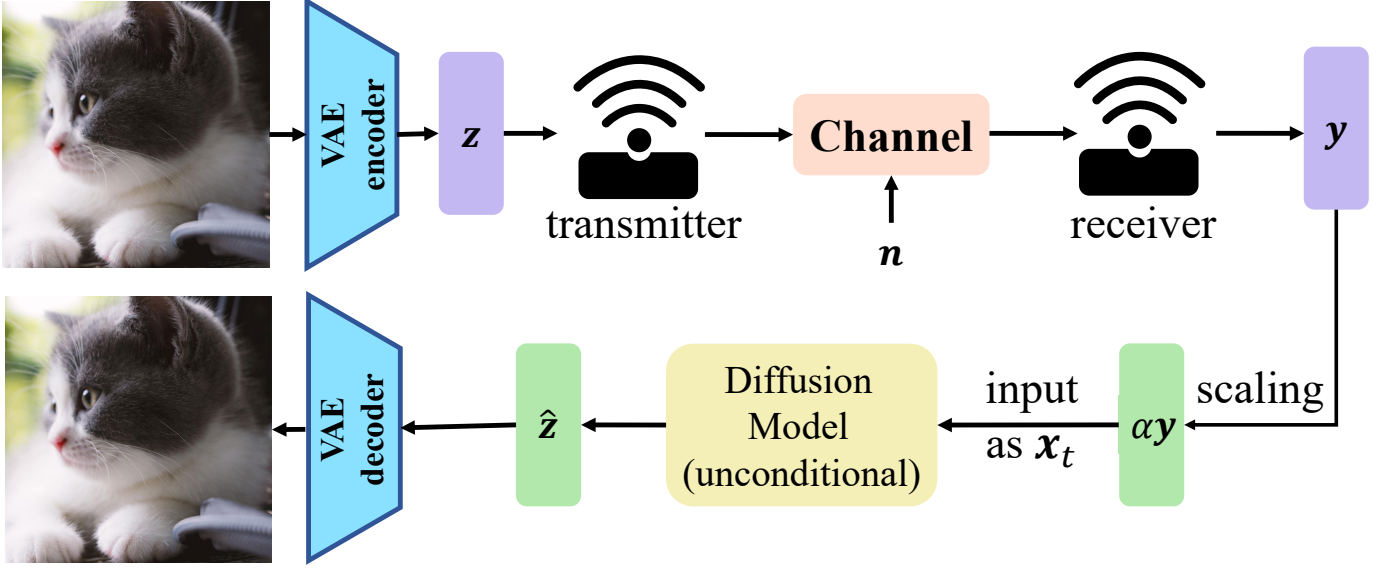


Fig. 1: Illustration of the proposed semantic communication framework.

from those observed during training. This leads to pronounced performance degradation under low-SNR or unexpected channel conditions [10]. Fundamentally, this vulnerability stems from a distribution mismatch between training and inference inputs, a phenomenon commonly referred to as the out-of-distribution (OOD) problem [11]. Moreover, the issue is further exacerbated by the intrinsic properties of latent semantic representations. Unlike explicit modalities such as images or audio, latent features are highly abstract, compactly encoded, and often reside in non-Euclidean manifolds [11]. This compressed structure renders them particularly fragile to perturbations. Even minor Gaussian noise interference can induce significant distributional shifts that compromise the underlying semantic structure. Consequently, neural decoders struggle to accurately reconstruct the original content, as they fail to extract meaningful patterns from perturbed latent vectors. This fragility of the latent space poses a unique challenge to semantic communication systems, namely, how to effectively model, diagnose, and mitigate noise-induced performance degradation in compressed semantic domains to improve the fidelity and reliability of the semantic feature decoding. Furthermore, current neural semantic systems are often tailored to data from a particular distribution, limiting their scalability to broader domains. When the distribution of transmitted data changes, even slightly, from the distribution of cats to the distribution of dogs, the performance of the system can deteriorate substantially, necessitating full retraining [2]. Such dependence on narrowly scoped training regimes not only impairs scalability but also introduces a prohibitive computational burden when deployed in dynamic or heterogeneous environments. Consequently, the lack of noise resilience, data generalization, and model adaptability remains a fundamental bottleneck that hinders the widespread application of neural network-based semantic communication in real-world 6G scenarios [12].

The aforementioned limitations arise from a deeper theoretical mismatch between the intrinsic nature of semantic

communication and the architectural foundations of current neural network-based solutions [11]. Traditional semantic communication frameworks predominantly adopt autoencoder-based architectures, where the neural backbone is trained in a discriminative manner. While effective in encoding data representations under matched training and inference conditions, such models exhibit a critical limitation: they lack the capacity to generate meaningful outputs from null or severely degraded inputs. This behavior is indicative of a discriminative modeling approach, which aims to extract discriminative features rather than to model the full data distribution. According to statistical learning theory, discriminative models are inherently restricted to learning decision boundaries or conditional mappings, rather than capturing the underlying generative process of the data. However, from an information-theoretic perspective, semantic communication aims to exploit the prior distribution of source data, which is the semantic information, to optimize source and channel encoding jointly. This joint design enables more efficient data compression and enhanced resilience against channel impairments. Crucially, without effective utilization of the data's prior distribution, it is fundamentally difficult to realize the theoretical performance gains of semantic communication. This insight motivates a paradigm shift from discriminative to generative modeling as the backbone architecture of semantic communication systems. Generative models, by construction, capture the underlying data distribution and therefore enable maximum a posteriori (MAP) estimation of corrupted semantic features, facilitating robust recovery of the original content from noisy observations. Although recent studies have proposed generative-model-based semantic communication frameworks, they often rely on conditional generative models that reconstruct data from transmitted semantic features. However, this approach suffers from two notable drawbacks. First, conditional generative models typically involve manually injected Gaussian noise during training to facilitate sampling. This artificial injection often leads to a mismatch between generated samples and the

true distribution of the original data, especially under noisy channel conditions. Second, these models generally depend on conditional encoders to extract semantic features. As previously noted, such encoders are essentially discriminative in nature, and are therefore vulnerable to OOD degradation when exposed to distorted features resulting from channel noise. To address these limitations, a new generative-model-driven framework is required—one that both eliminates the reliance on fragile conditional structures and fully leverages the inherent data priors learned by the generative model. Such a design would enable effective denoising and semantic reconstruction even under adverse channel conditions, thereby enhancing both the robustness and theoretical fidelity of semantic communication systems.

To address the above challenges, this work introduces a novel semantic communication architecture based on latent diffusion models (LDMs) [13]. The key innovation lies in leveraging the generative capability of LDMs to perform semantic-level denoising in the latent space of a variational autoencoder (VAE) framework [14]. Instead of directly operating in the high-dimensional signal domain, our method encodes semantic information into a compact latent representation, which is then transmitted over a noisy channel. Upon reception, the system applies an LDM to iteratively remove additive Gaussian noise from the corrupted latent features through a learned reverse diffusion process. This design enables robust semantic recovery even under severe SNR degradation, without requiring retraining for each noise condition. The theoretical foundation of this architecture is grounded in stochastic differential equations (SDE) theory, which formally describes the diffusion and denoising process as a continuous-time Markov chain driven by Brownian motion [15], [16]. In this framework, we derive a closed-form relationship between the SNR of the received feature map and the appropriate denoising timestep in the LDM. This mapping allows the receiver to adaptively select the number of reverse diffusion steps based on the observed channel conditions, ensuring that the generative denoising process is optimally matched to the level of corruption in the signal. Furthermore, to mitigate the OOD problem caused by mismatched input statistics, we introduce a linear scaling mechanism that transforms the received noisy latent features to align with the prior distribution assumed during the diffusion model’s training phase. The combination of adaptive timestep selection and input scaling endows the proposed architecture with strong generalization capabilities across a wide range of channel noise conditions. Crucially, since the LDM is decoupled from the encoder-decoder training pipeline and used solely for noise suppression, pre-trained diffusion models from general computer vision tasks can be directly integrated without fine-tuning. This plug-and-play property significantly reduces system design complexity and enables continual evolution of the communication system as more powerful generative models become available. By bridging stochastic process theory with semantic communication design, our approach provides both theoretical guarantees and practical robustness, paving the way for scalable, noise-resilient 6G communication systems. The main contributions of this paper are summarized as follows.

- 1) A novel theoretical foundation for semantic communication is established in this paper by leveraging SDEs to model the relationship between channel-induced Gaussian noise and the reverse diffusion process in generative models. We derive a closed-form analytical expression linking the signal-to-noise ratio (SNR) of the received semantic representation to the appropriate denoising timestep in the diffusion model. This formulation enables precise and adaptive noise mitigation without retraining, offering a mathematically grounded mechanism to handle arbitrary noise levels. The proposed theory not only bridges the gap between stochastic process modeling and neural semantic communication but also enhances robustness under out-of-distribution channel conditions, a longstanding challenge in the field.
- 2) Building on the above theoretical framework, we propose an end-to-end semantic communication system that integrates a VAE with an LDM. In this architecture, the VAE compresses high-dimensional source data into compact semantic latent variables, which are transmitted over a noisy channel and then denoised using a pretrained LDM. By introducing a scaling mechanism to align the noisy latent features with the training distribution of the LDM, the system effectively mitigates OOD issues. Crucially, the LDM operates independently of the encoder-decoder pipeline and can be replaced by any pretrained diffusion model, enabling zero-shot generalization across diverse SNRs and data types without task-specific fine-tuning.
- 3) Experiments

II. RELATED WORKS AND PRELIMINARIES

A. Semantic Communications

Semantic communication has emerged as a transformative paradigm in the evolution of next-generation wireless systems, particularly 6G, aiming to bridge the gap between signal transmission and meaning understanding. Unlike conventional Shannon-centric systems that prioritize bit-level fidelity, semantic communication seeks to transmit the intended meaning of messages effectively, thus aligning the communication process with the task-specific utility at the receiver. This paradigm shift has triggered intensive theoretical and practical exploration in recent years, resulting in a rich body of literature.

Foundational works such as those by [6], [17] established the conceptual framework for semantic communication, delineating the limitations of Shannon theory in capturing semantic and effectiveness layers of communication, and advocating for AI-integrated approaches. Subsequent surveys, including those by [18] and [19], have categorized enabling technologies such as knowledge-based reasoning, deep learning-based encoders, and task-oriented transmission frameworks. These reviews have also formalized key metrics including semantic entropy, semantic rate-distortion, and semantic channel capacity, marking a theoretical extension beyond classical information theory.

In parallel, significant efforts have been made toward system-level innovations. [20] and [21] reviewed emerging architectures that integrate semantic communication with deep joint source-channel coding (JSCC), generative AI, and federated learning.

These contributions underline the role of large language models (LLMs) and semantic knowledge bases (KBs) in enhancing interpretability, compressibility, and adaptability of semantic encoders across modalities such as text, image, audio, and video. The work by Lema et al. [22] highlights the convergence of semantic communication with edge computing and proposes scalable architectures for real-time, context-aware applications.

A number of domain-specific studies have investigated semantic communication across critical verticals. For instance, [23] examines its integration into vehicular networks (V2X), focusing on multimodal semantic extraction, cooperative coding, and dynamic resource allocation. Similarly, other works explore semantic transmission in metaverse platforms, Internet of Things (IoT), wireless sensor networks (WSN), and healthcare, emphasizing the ability to reduce bandwidth consumption and improve robustness through semantic compression and prediction. Despite these advances, several open challenges remain. Theoretical gaps persist in defining a unified framework for semantic information quantification and in establishing universal semantic performance metrics. Additionally, the issues of dynamic KB synchronization, adversarial robustness, interpretability of deep semantic models, and semantic-level security threats have become critical research frontiers. Recent studies, such as those by [24], have introduced performance modeling techniques, such as the Alpha-Beta-Gamma (ABG) expression, to bridge empirical deep learning performance with classical SNR-based communication analysis.

B. Diffusion Model

Diffusion models are a class of generative models that produce data samples by iteratively reversing a predefined noise-injection process. Originally proposed as an alternative to generative adversarial networks (GANs) [25], diffusion models have demonstrated remarkable performance in diverse generative tasks, including image synthesis, natural language modeling, and structured data generation [26], [27]. Beyond generation, they have also shown promise in perception-oriented applications such as image segmentation, object detection, and model-based reinforcement learning [13]. At their core, diffusion models define a two-stage process: a forward diffusion stage that incrementally perturbs input data with Gaussian noise, and a reverse denoising stage that reconstructs the data through a learned Markov process. Let \mathbf{x}_0 denote the clean input. The forward process generates latent variables $\mathbf{x}_1, \dots, \mathbf{x}_T$ via a Markov chain with Gaussian transitions as follows.

$$q(\mathbf{x}_t | \mathbf{x}_{t-1}) = \mathcal{N}(\sqrt{1 - \beta_t} \mathbf{x}_{t-1}, \beta_t \mathbf{I}), \quad (1)$$

where $\beta_t \in (0, 1)$ controls the noise variance at step t . By defining $\alpha_t = 1 - \beta_t$ and $\bar{\alpha}_t = \prod_{s=1}^t \alpha_s$, one obtains the closed-form marginal as follows.

$$q(\mathbf{x}_t | \mathbf{x}_0) = \mathcal{N}(\sqrt{\bar{\alpha}_t} \mathbf{x}_0, (1 - \bar{\alpha}_t) \mathbf{I}), \quad (2)$$

Applying the sampling rule, the following align can be obtained.

$$\mathbf{x}_t = \sqrt{\bar{\alpha}_t} \mathbf{x}_0 + \sqrt{1 - \bar{\alpha}_t} \boldsymbol{\epsilon}, \quad \boldsymbol{\epsilon} \sim \mathcal{N}(\mathbf{0}, \mathbf{I}). \quad (3)$$

The reverse process approximates the true posterior using a parameterized model $p_\theta(\mathbf{x}_{t-1} | \mathbf{x}_t)$, defined as follows.

$$p_\theta(\mathbf{x}_{t-1} | \mathbf{x}_t) = \mathcal{N}(\boldsymbol{\mu}_\theta(\mathbf{x}_t, t), \beta_t \mathbf{I}), \quad (4)$$

where $\boldsymbol{\mu}_\theta$ is a neural network trained to predict the denoised signal at each step. Sampling proceeds from $\mathbf{x}_T \sim \mathcal{N}(\mathbf{0}, \mathbf{I})$ down to \mathbf{x}_0 , with each denoising step computed as follows.

$$\mathbf{x}_{t-1} = \frac{1}{\sqrt{\alpha_t}} \left(\mathbf{x}_t - \frac{1 - \alpha_t}{\sqrt{1 - \bar{\alpha}_t}} \boldsymbol{\mu}_\theta(\mathbf{x}_t, t) \right) + \beta_t \mathbf{z}, \quad (5)$$

The final noise term ensures that the variance of the denoised sample aligns with that of the forward process. While a more precise formulation would scale this term using $\tilde{\beta}_t = \frac{1 - \bar{\alpha}_{t-1}}{1 - \bar{\alpha}_t} \beta_t$, empirical studies [28] have shown that using β_t directly provides a favorable trade-off between computational efficiency and denoising performance.

III. SYSTEM MODEL AND PROBLEM FORMULATION

We consider a semantic communication system that transmits high-level representations of source data through a noisy wireless channel, with the goal of reconstructing the intended semantic content at the receiver. Unlike traditional symbol-based communication systems, the focus here lies in end-to-end semantic fidelity rather than exact bit-level recovery.

The end-to-end system comprises a source, a joint source-channel encoder, an additive white Gaussian noise (AWGN) channel, a denoising module, and a decoder. Let $\mathbf{x} \in \mathbb{R}^n$ denote the original source data. The source encoder, parameterized by ϕ , maps \mathbf{x} into a compact semantic latent vector $\mathbf{z} \in \mathbb{R}^d$, with $d \ll n$, via

$$\mathbf{z} = f_\phi(\mathbf{x}), \quad (6)$$

where $f_\phi : \mathbb{R}^n \rightarrow \mathbb{R}^d$ is typically realized by a variational autoencoder (VAE). The semantic latent vector \mathbf{z} is transmitted over an AWGN channel, yielding the received representation

$$\tilde{\mathbf{z}} = \mathbf{z} + \mathbf{n}, \quad \mathbf{n} \sim \mathcal{N}(\mathbf{0}, \sigma^2 \mathbf{I}), \quad (7)$$

where σ^2 denotes the channel noise power.

At the receiver, the corrupted latent variable $\tilde{\mathbf{z}}$ undergoes denoising to mitigate the impact of channel noise. Let $g_\psi : \mathbb{R}^d \rightarrow \mathbb{R}^d$ represent the denoising function parameterized by ψ , and $h_\theta : \mathbb{R}^d \rightarrow \mathbb{R}^n$ denote the semantic decoder parameterized by θ . The final reconstructed data $\hat{\mathbf{x}}$ is obtained as

$$\hat{\mathbf{x}} = h_\theta(g_\psi(\tilde{\mathbf{z}})). \quad (8)$$

In conventional systems, g_ψ may be a simple denoising autoencoder trained under a fixed SNR regime. However, such systems are inherently sensitive to variations in noise and data distribution, often resulting in suboptimal performance under mismatched conditions. In contrast, the proposed architecture adopts a pretrained LDM as g_ψ , offering a generative and noise-adaptive alternative.

The design objective is to minimize the semantic distortion between the reconstructed output $\hat{\mathbf{x}}$ and the ground truth input \mathbf{x} . A natural choice of loss function is the mean squared error (MSE):

$$\min_{\phi, \psi, \theta} \mathbb{E}_{\mathbf{x}, \mathbf{n}} [\|\mathbf{x} - h_\theta(g_\psi(\mathbf{z} + \mathbf{n}))\|^2], \quad (9)$$

subject to the encoder constraint $z = f_\phi(x)$. This formulation captures the full stochasticity of the channel and reflects the end-to-end performance of the semantic transmission process. Two primary challenges arise in solving this problem. First, due to the dimensionality reduction $d \ll n$, the decoder must reconstruct a high-dimensional signal from a compressed and noise-contaminated latent representation. This makes the inverse mapping severely ill-posed and sensitive to noise perturbations. Second, the Gaussian noise introduced during transmission alters the distribution of the latent variable at the receiver, causing a significant mismatch between the training and inference distributions, commonly referred to as the OOD problem. These challenges underscore the need for a robust, distribution-aware denoising mechanism that can generalize across varying SNRs and input distributions. To address this, we propose a theoretically grounded denoising approach based on stochastic differential aligns and generative diffusion models, which will be detailed in the next section.

IV. DIFFUSION BASED SEMANTIC COMMUNICATION FRAMEWORK

A. Theoretical Basis of Diffusion Model-Based Denoising

DM enables high-fidelity data generation and denoising by simulating a stochastic process that gradually perturbs structured data into noise and then learns to reverse this process. While originally formulated as a discrete Markov chain, recent advances have shown that the diffusion process can also be interpreted as a continuous-time SDE, providing a principled framework for both theoretical analysis and practical acceleration.

Following the framework of [15], the forward diffusion process can be equivalently represented as an Itô SDE of the form:

$$d\mathbf{x}_t = f_t \mathbf{x}_t dt + g_t d\mathbf{w}_t, \quad (10)$$

where $\mathbf{x}_t \in \mathbb{R}^d$ denotes the latent variable at time $t \in [0, T]$, \mathbf{w}_t is a standard Wiener process, f_t is a time-dependent drift coefficient, and g_t is the diffusion coefficient. For tractability, we set $g_t = 1$ and define the drift as $f_t \mathbf{x}_t = \mathbf{h}_t$, yielding the integral representation:

$$\mathbf{x}_t = \mathbf{x}_0 + \int_0^t \mathbf{h}_s ds + \int_0^t d\mathbf{w}_s. \quad (11)$$

Under this formulation, the conditional distribution of \mathbf{x}_t given the initial state $\mathbf{x}_0 \sim q(\mathbf{x}_0)$ is Gaussian:

$$q(\mathbf{x}_t | \mathbf{x}_0) = \mathcal{N}\left(\mathbf{x}_t; \mathbf{x}_0 + \int_0^t \mathbf{h}_s ds, t\mathbf{I}\right). \quad (12)$$

Alternatively, this can be expressed as follows

$$\mathbf{x}_t = \mathbf{x}_0 + \int_0^t \mathbf{h}_s ds + \sqrt{t}\boldsymbol{\epsilon}, \quad \boldsymbol{\epsilon} \sim \mathcal{N}(\mathbf{0}, \mathbf{I}). \quad (13)$$

Since the \mathbf{h}_t holds $\int_0^1 \mathbf{h}_t + \mathbf{x}_0 = 0$, a simplified expression of (13) can be obtained as follows.

$$\mathbf{x}_t = (1 - t)\mathbf{x}_0 + \sqrt{t}\boldsymbol{\epsilon}. \quad (14)$$

To recover the original clean latent representation \mathbf{x}_0 from the noisy variable \mathbf{x}_t , the reverse-time SDE is formulated as follows.

$$d\mathbf{x}_t = \left[f_t \mathbf{x}_t - \frac{g_t^2}{\beta_t} \boldsymbol{\epsilon}_t \right] dt + g_t d\bar{\mathbf{w}}_t, \quad (15)$$

where $\bar{\mathbf{w}}_t$ is an independent Wiener process and $\boldsymbol{\epsilon}_t$ represents the perturbation introduced during the forward process, scaled by the noise schedule β_t . Setting $f_t \mathbf{x}_t = \mathbf{h}_t$ and $g_t = 1$ yields a simplified expression of the reverse-time transition. In discrete time, this reverse process can be approximated as follows.

$$\mathbf{x}_{t-\Delta t} = \mathbf{x}_t + \int_t^{t-\Delta t} \mathbf{h}_s ds - \frac{\Delta t}{t} \boldsymbol{\epsilon} + \sqrt{\frac{\Delta t(t-\Delta t)}{t}} \tilde{\boldsymbol{\epsilon}}, \quad (16)$$

where $\boldsymbol{\epsilon} \sim \mathcal{N}(\mathbf{0}, \mathbf{I})$ corresponds to the forward noise term and $\tilde{\boldsymbol{\epsilon}} \sim \mathcal{N}(\mathbf{0}, \mathbf{I})$ is a newly added Gaussian noise for variance matching in the reverse step. These noise terms are statistically independent, reflecting the stochastic symmetry of the diffusion process.

From (16), it is evident that the success of denoising hinges on the accurate estimation of the drift term \mathbf{h}_t and the forward noise $\boldsymbol{\epsilon}$. In practice, modern denoising diffusion models train neural networks to predict either \mathbf{h}_t directly (as in score-based generative modeling) or the noise term $\boldsymbol{\epsilon}$ added during the forward process. The predicted value is then used to guide the reverse sampling path from \mathbf{x}_T to \mathbf{x}_0 . The feasibility of this prediction is supported by the universal approximation theorem, which guarantees that a sufficiently expressive neural network can approximate the mappings required for effective denoising. State-of-the-art systems such as Stable Diffusion and DALL-E rely on this principle to reconstruct high-dimensional images from noise, demonstrating the practical effectiveness of neural diffusion-based inference.

Remark 1. An important practical insight that arises from (16) is that if the denoising step size is chosen as $\Delta t = t$, then a single-step denoising operation can be performed. In this case, the denoised sample \mathbf{x}_0 is obtained in one step as follows.

$$\mathbf{x}_0 = \mathbf{x}_t - \boldsymbol{\epsilon} + 0 \cdot \tilde{\boldsymbol{\epsilon}}. \quad (17)$$

This enables fast inference, where the diffusion model's computational latency becomes comparable to that of traditional neural network-based denoisers. In scenarios such as semantic communication, this property is crucial for real-time or low-latency transmission requirements.

B. Relationship Between Diffusion Variable and Noisy Receiving

Although DMs are predominantly used for generative tasks, their fundamental mechanism is grounded not in predicting future data states but in estimating the Gaussian noise that corrupts them. Rather than producing $\mathbf{x}_{t-\Delta t}$ directly from \mathbf{x}_t , the neural network within the DM is trained to infer the noise component added between these two states. This denoising-centric formulation underlies their formal designation as denoising diffusion probabilistic models [28], and has proven

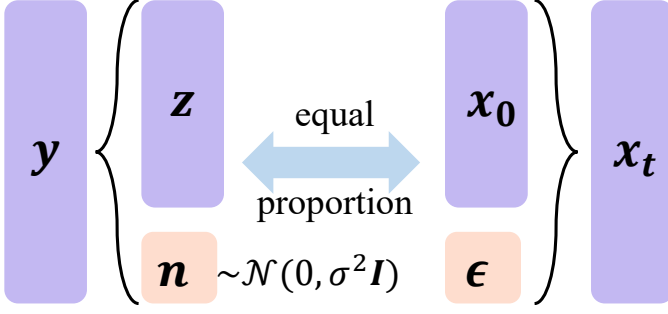


Fig. 2: Illustration of the denoising timestep calculation.

highly effective in reconstructing clean data across a range of applications. Importantly, the denoising process need not begin from pure Gaussian noise as $t = 1$. In practice, training is conducted over randomly sampled timesteps $t \in (0, 1]$, where the model learns to predict the noise corresponding to each level of corruption. As a result, DMs are inherently capable of initiating the reconstruction process from any intermediate noisy observation x_t , making them flexible tools for tasks beyond generation.

From the perspective of semantic communication, this flexibility necessitates careful consideration of how the denoising timestep t should be selected. As described in (14), the relative contributions of signal and noise in x_t are directly controlled by t . Larger values of t correspond to higher noise content and diminished signal presence, whereas smaller t values imply a cleaner input. If the timestep is mismatched to the actual corruption level, such as using a large t for lightly corrupted data, useful semantic features may be lost. Conversely, initiating denoising from a small t in the presence of severe noise may yield suboptimal results due to insufficient correction. To address this, we introduce an SNR-based strategy to align the timestep t with the statistical characteristics of the received signal. The rationale draws from an analogy to classical detection theory: just as signal recovery aims to extract the deterministic component z from a noisy observation y , diffusion denoising seeks to recover x_0 from x_t . Therefore, as is shown in Fig. 2, we propose that the optimal denoising performance can be achieved when the energy ratio between signal and noise in x_t is matched to that in y , thereby guiding the selection of t based on the estimated SNR. The t can be calculated as Theorem 1 and Remark 3.

Theorem 1. Assuming the $\mathbb{E}[\|x_0\|^2] = \gamma$, for any given received noisy latent feature map y , and noise density σ^2 of noisy channel, when

$$t = \frac{2 + \phi - \sqrt{\phi^2 + 4\phi}}{2}, \quad (18)$$

where $\phi = \frac{\mathbb{E}[\|y\|^2] - \sigma^2}{\gamma\sigma^2}$. The following equation can be obtained.

$$\frac{\mathbb{E}[\|z\|^2]}{\mathbb{E}[\|n\|^2]} = \frac{\mathbb{E}[\|(1-t)x_0\|^2]}{\mathbb{E}[\|\sqrt{t}\epsilon\|^2]}. \quad (19)$$

Proof. Because z and n are uncorrelated, their energies add: $\mathbb{E}[\|y\|^2] = \mathbb{E}[\|z\|^2] + \sigma^2$. Therefore, the following equation

can be obtained.

$$\text{SNR}_{\text{obs}} = \frac{\mathbb{E}[\|y\|^2] - \sigma^2}{\sigma^2} = \frac{\mathbb{E}[\|z\|^2]}{\sigma^2} = \frac{(1-t)^2\gamma}{t}. \quad (20)$$

Introduce $\phi \triangleq \text{SNR}_{\text{obs}}/\gamma > 0$; the matching condition can be obtained as follows.

$$(1-t)^2 = \phi t. \quad (21)$$

Expanding yields the following equation.

$$t^2 - (2 + \phi)t + 1 = 0. \quad (22)$$

The discriminant is $(2 + \phi)^2 - 4 = \phi^2 + 4\phi > 0$, ensuring two real roots as follows.

$$t_{\pm} = \frac{2 + \phi \pm \sqrt{\phi^2 + 4\phi}}{2}. \quad (23)$$

Because $\phi > 0$, the “plus” root satisfies $t_+ > 1$ and violates the physical constraint $t < 1$; consequently it is rejected. The “minus” root can be obtained as follows.

$$t^* = t_- = \frac{2 + \phi - \sqrt{\phi^2 + 4\phi}}{2}. \quad (24)$$

□

Remark 2. According to Theorem 1, consider the mapping $g(t; \phi) \triangleq (1-t)^2 - \phi t$, $t \in [0, 1]$. Then the following properties hold. (1) For every $\phi \geq 0$ the equation $g(t; \phi) = 0$ admits a unique solution; (2) The function $t^*(\phi)$ is strictly decreasing in ϕ ; equivalently, t^* increases as SNR_{obs} decreases; (3) When $\text{SNR} \rightarrow 0$, $t = 1$ which equals to denoise from a total noise according to (14), and when $\text{SNR} \rightarrow +\infty$, $t = 0$ which means no denoise is needed.

Proof. Observing that $g(0; \phi) = 1 > 0$ and $g(1; \phi) = -(\phi) \leq 0$ for every $\phi \geq 0$, and noting the equation as follows.

$$\frac{\partial g}{\partial t} = 2(t-1) - \phi \quad (25)$$

$$\frac{\partial^2 g}{\partial t^2} = 2 > 0, \quad (26)$$

the $g(\cdot; \phi)$ is strictly convex on $[0, 1]$. A strictly convex function that changes sign exactly once on a closed interval possesses one and only one root; hence, the solution exists and is unique in $(0, 1]$. Solving $g(t; \phi) = 0$ yields the explicit closed-form root displayed above, whose radicand $\phi^2 + 4\phi = \phi(\phi + 4)$ is non-negative for all $\phi \geq 0$; consequently the square root is real and non-negative, ensuring t^* is well defined.

To establish monotonicity, differentiate t^* with respect to ϕ is as follows.

$$\frac{dt^*}{d\phi} = \frac{1 - \frac{1}{2}(2\phi + 4)/\sqrt{\phi^2 + 4\phi}}{2} < 0, \quad (27)$$

$$\forall \phi > 0, \quad (28)$$

because $2\phi + 4 > 0$ and $\sqrt{\phi^2 + 4\phi} > \phi$. Thus t^* decreases strictly with increasing ϕ . Finally, the limiting values follow directly from L'Hospital's rule applied to the closed-form expression [29]. As $\text{SNR}_{\text{obs}} \rightarrow \infty$ we have $\phi \rightarrow \infty$ and therefore $t^* \sim 1/\phi \rightarrow 0$, indicating that an infinitely clean observation requires no diffusion denoising. Conversely, when

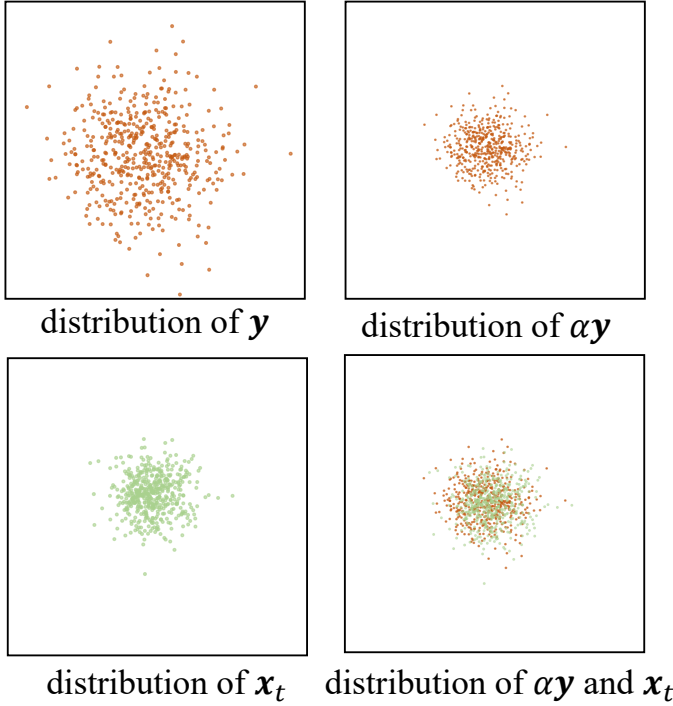


Fig. 3: Illustration of the scaling method.

$\text{SNR}_{\text{obs}} \rightarrow 0$ we obtain $\phi \rightarrow 0$ and $t^* \rightarrow 1$, meaning the denoiser must start from pure noise because the observation contains no discernible signal component. \square

Remark 3. In the training procedure, since the purpose of denoise is to solve \mathbf{z} , thus the \mathbf{x}_0 is set equal to \mathbf{z} . Therefore, the t can be simplified as follows.

$$t = \frac{2\sigma^2 + 1 - \sqrt{1 + 4\sigma^2}}{2\sigma^2}. \quad (29)$$

The absence of an explicit \mathbf{z} term in Remark 3 follows directly from the standard training protocol of diffusion models: during pre-training, the latent signal energy is normalised to a fixed range, which is equivalent to assuming a constant transmit power. Under this normalisation, the instantaneous SNR is governed solely by the additive-noise variance σ^2 . Consequently, the closed-form expression in Remark 3 depends only on σ^2 and no longer involves \mathbf{z} , yielding a simplified yet general mapping between the channel noise level and the optimal denoising timestep.

Theorem 1 guarantees the existence of a timestep $t \in (0, 1]$ for which the signal-noise ratio embedded in the diffusion variable \mathbf{x}_t exactly matches that of the received vector \mathbf{y} . However, during the training procedure, the DM is exposed only to pairs $(\mathbf{x}_0, \mathbf{x}_t)$ generated via the forward process in (14). Consequently, the network learns the statistics of \mathbf{x}_t rather than those of the true channel output. If \mathbf{y} is fed directly into the DM, the mismatch in input distribution leads to an OOD condition and a marked degradation in denoising accuracy, as is shown in Fig. 3. In wireless reception, this discrepancy can be reconciled by a simple power-normalisation step. Because both \mathbf{x}_t and \mathbf{y} are linear combinations of a deterministic term \mathbf{z} and zero-mean Gaussian noise, their distributional forms are identical up to second-order moments. Letting $\mathbf{x}_0 = \mathbf{z}$, we equalise

the average energies of \mathbf{y} and \mathbf{x}_t through a scalar factor α , i.e., $\mathbf{y}' = \alpha\mathbf{y}$. Selecting α according to Theorem 2 aligns the second-order statistics of \mathbf{y}' with those of \mathbf{x}_t , thereby ensuring that the pretrained DM operates within its learned distribution. This linear scaling not only restores denoising performance but also guarantees that the recovered latent vector coincides with the desired signal component \mathbf{z} without further post-processing.

Theorem 2. Define the scaled observation $\tilde{\mathbf{y}} = \alpha\mathbf{y}$ with scalar $\alpha > 0$. The equality

$$\mathbb{E}[\|\tilde{\mathbf{y}}\|^2] = \mathbb{E}[\|\mathbf{x}_t\|^2],$$

holds if and only if

$$\alpha = \sqrt{\frac{(1-t)^2(\mathbb{E}[\|\mathbf{y}\|^2] - \sigma^2) + t}{\mathbb{E}[\|\mathbf{y}\|^2]}} = \sqrt{\frac{(1-t)^2\gamma + t}{\gamma + \sigma^2}}. \quad (30)$$

Moreover, $0 < \alpha \leq 1$; α decreases strictly with t and with the observable signal-to-noise ratio $S = (\mathbb{E}[\|\mathbf{y}\|^2] - \sigma^2)/\sigma^2$.

Proof. Because \mathbf{z} and \mathbf{n} are uncorrelated, $\mathbb{E}[\|\mathbf{y}\|^2] = \gamma + \sigma^2 = \mathbb{E}[\|\mathbf{y}\|^2]$. Scaling by α multiplies the second-order moment by α^2 , hence

$$\mathbb{E}[\|\tilde{\mathbf{y}}\|^2] = \alpha^2 \mathbb{E}[\|\mathbf{y}\|^2]. \quad (31)$$

Equating the above to the target power $(1-t)^2\gamma + t$ and substituting $\gamma = \mathbb{E}[\|\mathbf{y}\|^2] - \sigma^2$ derived from the observable statistics yields the follows.

$$\alpha^2 \mathbb{E}[\|\mathbf{y}\|^2] = (1-t)^2(\mathbb{E}[\|\mathbf{y}\|^2] - \sigma^2) + t, \quad (32)$$

$$\alpha^2 = \frac{(1-t)^2(\mathbb{E}[\|\mathbf{y}\|^2] - \sigma^2) + t}{\mathbb{E}[\|\mathbf{y}\|^2]}. \quad (33)$$

Taking the principal square root preserves positivity and furnishes the closed form for α . Positivity follows from $t \in (0, 1)$ and $\mathbb{E}[\|\mathbf{y}\|^2] > \sigma^2$. To bound α by unity, observe that $(1-t)^2(\mathbb{E}[\|\mathbf{y}\|^2] - \sigma^2) + t \leq \mathbb{E}[\|\mathbf{y}\|^2]$ because $(1-t)^2 \leq 1-t$ on $(0, 1)$ and $t < 1$. Strict decrease in t is evident from the negative derivative of the numerator with respect to t ; strict decrease in S follows from the monotonic growth of $\mathbb{E}[\|\mathbf{y}\|^2]$ with γ . \square

A direct consequence of Theorem 1 and Theorem 2 is that the properly rescaled observation $\tilde{\mathbf{y}} = \alpha\mathbf{y}$ attains the *same second-order distribution* as the synthetic sample \mathbf{x}_t employed during diffusion training. Because the clean component of the channel output equals the training datum ($\mathbf{z} = \mathbf{x}_0$), the only mismatch between the two random vectors is the pair of linear coefficients that multiplies the signal term and the additive Gaussian term, respectively. Selecting the step size t via Theorem 1 ensures that the signal-to-noise ratio satisfies $(1-t)^2\gamma/t = \gamma/\sigma^2$; the ensuing scaling factor derived in Theorem 3 simplifies to $\alpha^2 = t/\sigma^2$, so that $\alpha\mathbf{y} = (1-t)\mathbf{x}_0 + \sqrt{t}\hat{\epsilon}$ with $\hat{\epsilon} \sim \mathcal{N}(\mathbf{0}, \mathbf{I})$. Therefore the rescaled received vector replicates exactly the affine stochastic structure of \mathbf{x}_t . Although $\gamma = \mathbb{E}[\|\mathbf{x}_0\|^2]$ appears in both theorems, it is known at training time because it can be replaced by the empirical mean energy $\bar{\gamma}$ computed over the entire corpus of clean samples. In summary, the pair $\{t^*, \alpha^*\}$ aligns the second-order statistics—and, when

\mathbf{x}_0 is Gaussian, the full distribution—of the real channel observation with those of the diffusion-generated surrogate, thereby allowing the denoiser trained on \mathbf{x}_t to operate on actual channel outputs without retraining or additional calibration.

C. LDM Based Sematic Communciation Framework

To enable robust semantic communication over noisy channels, we propose an enhanced receiver architecture that integrates a pretrained LDM for adaptive denoising within the latent space, as shown in Fig. 1. Building upon the system model described earlier, the key novelty lies in the use of a generative denoising process that is aware of SNR and dynamically adapts to the characteristics of the received latent representation.

Given the received latent vector $\tilde{\mathbf{z}} = \mathbf{z} + \mathbf{n}$, where \mathbf{z} denotes the transmitted latent semantic representation and $\mathbf{n} \sim \mathcal{N}(0, \sigma^2 \mathbf{I})$ represents channel noise, the receiver first estimates the instantaneous SNR. This estimate is used to analytically determine a denoising timestep $t \in (0, 1]$ according to Theorem 1, which ensures that the signal-noise energy ratio in the diffusion variable matches that of the channel output. Simultaneously, a linear scaling factor α is computed via Theorem 2 to adjust the received vector’s magnitude, aligning its distribution with that of the diffusion model’s training inputs. This transformation yields the input to the LDM as $\mathbf{x}_t = \alpha \mathbf{y}$. The LDM then performs reverse diffusion starting from $\alpha \mathbf{y}$, using the analytically determined timestep t from Theorem 1. Different from conventional denoisers, which are often retrained or fine-tuned under new noise conditions, the LDM leverages its learned generative prior to adapt across a wide range of channel perturbations without modification. The reverse process can be executed with a variable number of iterations, depending on the SNR: fewer steps under high-quality channels and more when the received signal is severely corrupted. In particular, the framework supports single-step reverse inference using the approximated expression in (16), which enables low-latency operation when appropriate. Once denoised, the output $\hat{\mathbf{z}}$ is forwarded to the decoder, which reconstructs the semantic data. Since the LDM operates in latent space, its computational burden is low compared to pixel- or token-level generative models. Furthermore, the use of pretrained LDMs decouples the denoising mechanism from the encoder-decoder training, enabling modular updates. That is, more powerful LDMs—trained on large-scale data or advanced architectures—can be integrated directly, enhancing performance without altering the underlying semantic transceiver structure. This modular, SNR-aware framework allows the semantic communication system to maintain robustness against varying channel conditions while retaining the scalability and efficiency of a latent-space representation. It overcomes the limitations of conventional discriminative models, which suffer from generalization gaps when encountering unseen noise levels or out-of-distribution inputs, by grounding the denoising process in the theoretical structure of stochastic differential equations and distribution alignment.

V. EXPERIMENT RESULTS

A. Datasets and Evaluation Metrics

To evaluate the effectiveness of the proposed LDM-based semantic communication framework, we conducted extensive experiments on the CelebA-HQ dataset, a large-scale, high-resolution facial image corpus widely used for image generation and reconstruction tasks. As baseline comparisons, we selected two representative deep joint source-channel coding (JSCC) methods as follows. **Deep JSCC** [30], a classical convolutional architecture for image transmission, and **Swin JSCC** [31], a state-of-the-art transformer-based semantic communication model known for its superior performance on vision tasks. In addition, we included **stable diffusion (SD)** [13] as a generative baseline to assess the denoising capability of pretrained diffusion models in a semantic communication context. Specifically, the VAE in SD was utilized to perform joint source-channel encoding, analogous to the structure of the proposed LDM-based architecture. The corrupted latent features resulting from channel transmission were used as conditional inputs to the SD model, accompanied by a fixed textual prompt: “generate a clean and noise-free latent feature based on the content of this latent feature.” This prompt guided the model to perform direct semantic denoising using its pretrained generative prior. For our framework, we employed a pretrained latent diffusion model trained jointly on the CelebA-HQ [32] and ImageNet [33] datasets, without any task-specific fine-tuning or post-training being applied, thereby highlighting the generalizability and zero-shot capability of the proposed architecture. To comprehensively assess reconstruction quality, we adopted both pixel-level and semantic-level evaluation metrics. Quantitatively, root mean squared error (RMSE) was used to measure pixel-wise distortion. Additionally, we evaluated semantic preservation and perceptual quality using peak signal-to-noise ratio (PSNR), structural similarity index measure (SSIM) [34], and learned perceptual image patch similarity (LPIPS) [35]. These metrics collectively reflect the system’s fidelity in both low-level accuracy and high-level semantic consistency.

B. Performance Comparison on CelebA-HQ

The qualitative and quantitative performance of the proposed LDM-based semantic communication framework is illustrated in Fig. 4-6. Fig. 5 presents visual comparisons of image reconstruction outcomes under varying SNR conditions. It is evident that the proposed method achieves superior restoration quality, even under severely degraded channel conditions. Notably, without any task-specific fine-tuning, the LDM-based approach consistently preserves semantic structure and fine-grained details across a broad SNR range. In contrast, the two baseline deep JSCC methods demonstrate significant degradation under low SNRs, manifesting in blurry textures and distorted geometries. While the Swin-JSCC architecture performs better at low SNRs and can generate relatively clean outputs, its reconstructions tend to be overly smooth, with visibly diminished detail fidelity. This smoothness suggests a loss of high-frequency semantic features, likely due to the reliance on discriminative learning mechanisms, which are

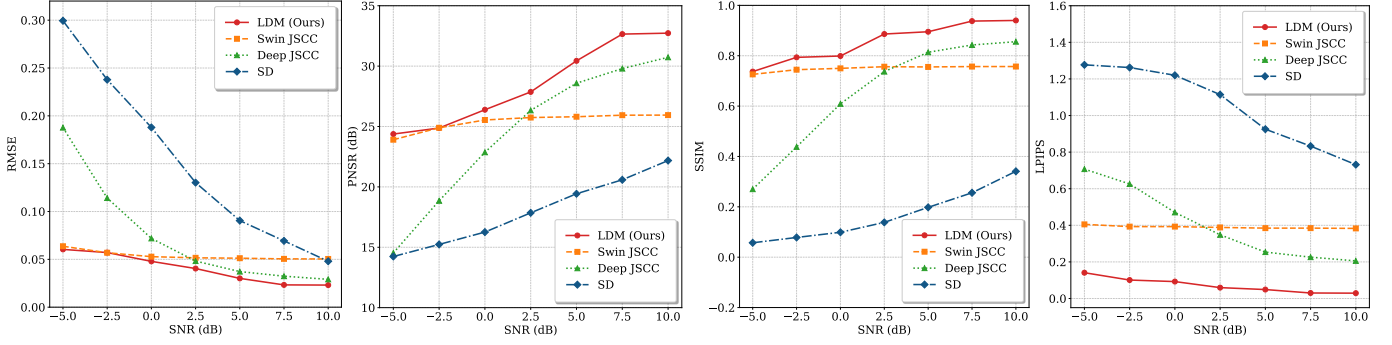


Fig. 4: Performance evaluation of different methods on various SNRs in the CelebA-HQ datasets.

Method \ SNR	GT	10 dB	7.5 dB	5.0 dB	2.5 dB	0.0 dB	-2.5 dB	-5.0 dB
Deep JSCC								
Swin JSCC								
SD								
LDM (Ours)								

Fig. 5: Comparison of image transmission performance at different SNR.

vulnerable to OOD channel perturbations and lack the capacity for generative recovery of corrupted latent semantics. We also evaluated a SD-based approach, where the received noisy latent features were used as conditional inputs alongside a denoising prompt. Despite this prompt-driven guidance, the SD model failed to produce competitive results, primarily because it was never explicitly trained to perform conditional denoising in the latent space. As a result, the generated outputs exhibited structural inconsistencies and semantic drift. The effectiveness of the LDM-based approach is further validated in Fig. 4, which summarizes numerical performance across a wide range of SNRs. The proposed method outperforms all baselines in both pixel-level fidelity, which is measured by RMSE, and semantic similarity metrics, including PSNR, SSIM, and LPIPS. Of particular note is the system’s behavior in low-SNR regimes, such as $\text{SNR} < 0\text{ dB}$, the degradation trends of all evaluation metrics flatten considerably for the LDM-based framework, indicating strong resilience to severe channel noise. Fig. 6 further substantiates this robustness by showcasing restored outputs at -10 dB and -20 dB SNRs. Even at -10 dB , the proposed system preserves most visual and structural semantics, and at -20 dB , although fine-grained object details may be lost, high-level semantic attributes—such as facial orientation and gender identity—remain correctly reconstructed. These results highlight the LDM’s unique ability

to capture and restore abstract semantic content under extreme channel impairments, demonstrating its advantage over both discriminative and conditional generative baselines.

C. Performance Demonstration of OOD Data

In addition to the semantic distortion caused by additive noise in the communication channel, semantic communication systems also face a more fundamental and often overlooked challenge: OOD generalization with respect to the transmitted data itself. While the majority of existing semantic communication research focuses on the robustness of latent feature recovery under noise, the problem of distributional shift between training data and real-world test data has received comparatively limited attention. In practice, semantic communication systems are often trained on specific datasets using supervised end-to-end learning pipelines, such as those adopted in classical Deep JSCC [30] and Swin-JSCC [31] frameworks. Although these systems may achieve excellent reconstruction performance on in-distribution samples, their ability to generalize across diverse data distributions remains highly constrained. To empirically validate this limitation, we follow standard training protocols and train several semantic transceivers, including Deep JSCC and Swin JSCC, on the CelebA-HQ dataset—a high-resolution portrait dataset. We then evaluate their performance on semantically unrelated image

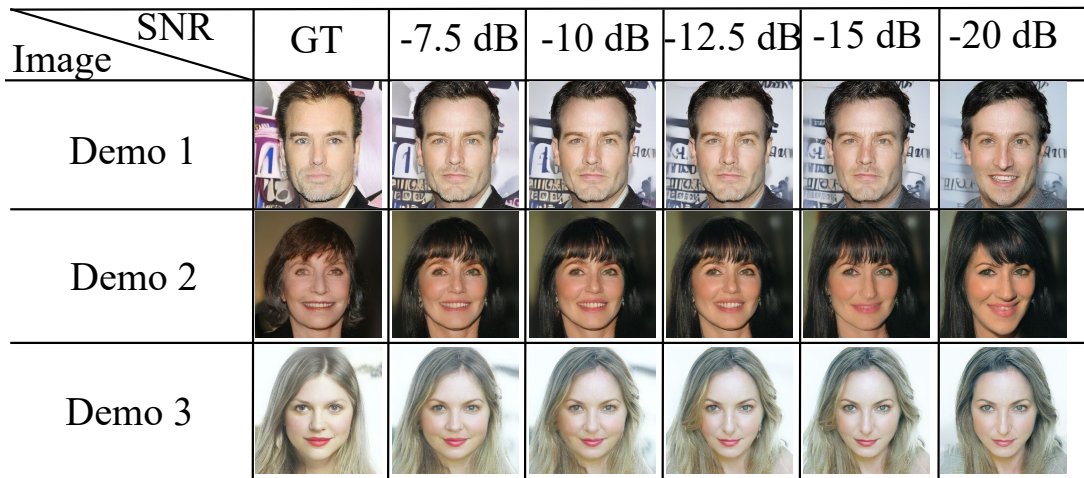


Fig. 6: The image transmission performance of the proposed method on low SNRs.

categories, including natural landscapes and animal scenes. As illustrated in Fig. 7 Deep JSCC exhibits significant degradation under OOD conditions, particularly when the channel SNR drops below 0dB. The reconstructed outputs suffer from both structural distortions and semantic ambiguity. Although Swin JSCC demonstrates improved low-SNR performance, it exhibits signs of overfitting to the portrait domain: when applied to landscape or animal images, the outputs are dominated by unnatural human-like textures, regardless of the original content. This over-specialization severely limits its applicability to real-world communication scenarios, where data distributions are often nonstationary and diverse. Interestingly, we observe that the SD model, though not optimized for end-to-end transmission, is still capable of preserving coarse semantic information, such as global shapes and object silhouettes, across different content types. This behavior is attributed to its training on large-scale, heterogeneous datasets such as LAION and ImageNet, which enables the model to learn a generalizable representation of natural images. However, due to the lack of explicit training for channel noise suppression, the SD model struggles to recover detailed features or suppress semantic corruption introduced by the channel.

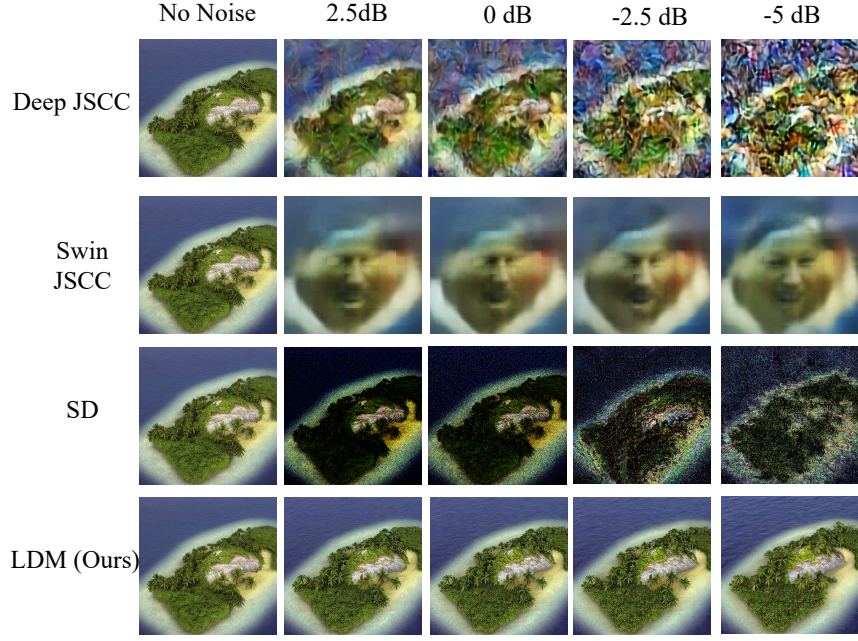
In contrast, the proposed LDM-based semantic communication framework directly addresses both noise robustness and data distribution generalization. By design, it decouples source-channel encoding from denoising and reconstruction, employing a pretrained LDM as a universal noise suppressor. A key advantage of our architecture is its modularity: the LDM component can be readily replaced with publicly available weights trained on large-scale datasets such as ImageNet or OpenImages. Without any task-specific fine-tuning, the system is capable of adapting to a wide range of visual domains. This makes it particularly well-suited for deployment in open-world communication environments where training data may not reflect future transmission requirements. Furthermore, because the LDM operates in the latent space of a VAE encoder, it preserves compactness and scalability while still benefiting from the rich generative priors of large-scale diffusion models. This plug-and-play compatibility with

open-source generative backbones imbues the system with a self-evolutionary capacity—as more powerful generative models become available, they can be directly integrated into the communication pipeline to enhance performance without retraining the encoder or decoder. In summary, the proposed framework not only resolves the vulnerability of semantic communication systems to channel-induced feature corruption, but also significantly improves cross-domain generalization through its integration with generative artificial intelligence. The ability to support robust semantic reconstruction under both SNR degradation and distributional shift underscores the practical utility and scalability of our approach for next-generation communication systems.

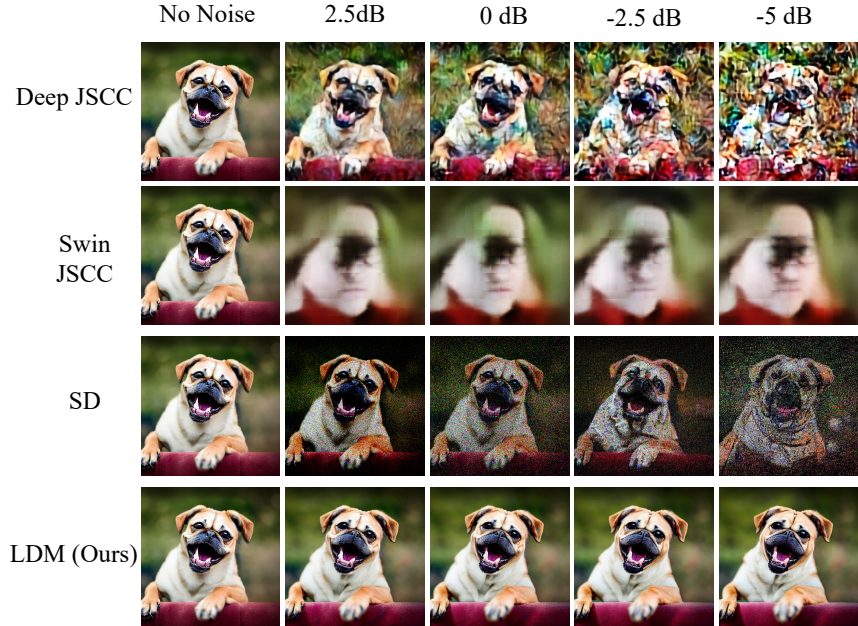
D. Numerical Proof of Theorem 1 and 2

To substantiate the theoretical claims made in Theorems 1 and 2 regarding the optimal denoising timestep t and scaling factor α , we perform a comprehensive numerical evaluation to assess their impact on end-to-end semantic reconstruction performance. Specifically, we aim to verify whether the closed-form expressions derived for t and α , which are analytically linked to the SNR and data distribution statistics, indeed correspond to optimal operational points in practice. In this experiment, we compare the performance of our LDM-based semantic communication framework under four different evaluation metrics: RMSE, peak PSNR, SSIM, and LPIPS. We systematically perturb the analytically computed values of t and α by $\pm 5\%$, $\pm 10\%$, $\pm 20\%$, and $\pm 50\%$ to simulate scenarios where the SNR is inaccurately estimated or where the parameter selection deviates from the ideal theoretical value. These perturbations are intended to reflect practical conditions, where perfect knowledge of channel statistics may not be available.

Fig. 8 illustrates the impact of these deviations in t on system performance. Across all metrics, the best results are consistently achieved when using the theoretically derived value of t . As the deviation increases, a clear monotonic degradation in performance is observed. This empirical behavior aligns with our theoretical expectation: the denoising performance of the



(a) Performance demonstration on OOD data of landscape.



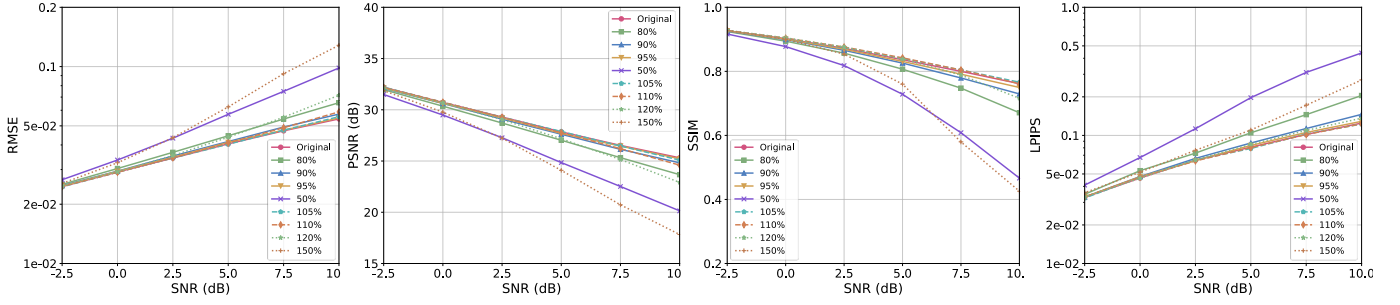
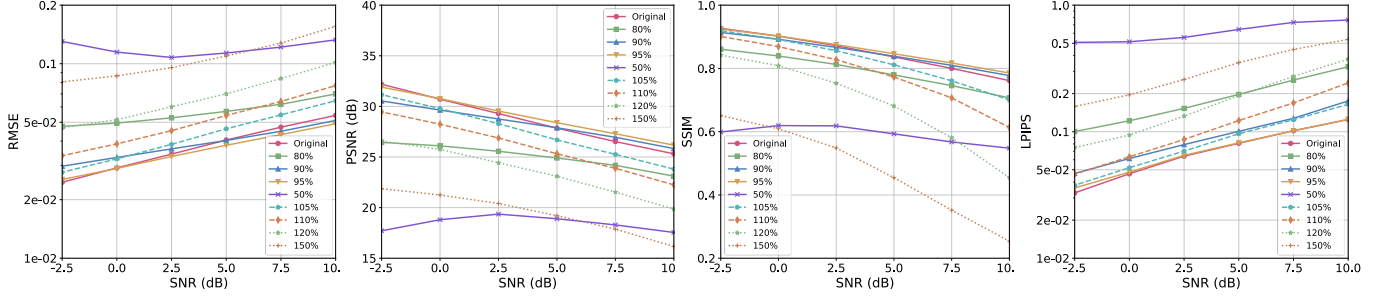
(b) Performance demonstration on OOD data of animal.

Fig. 7: Performance demonstration on OOD data.

diffusion model is highly sensitive to the matching between the true noise content and the chosen diffusion timestep. The further the assumed timestep diverges from the one that corresponds to the actual SNR, the more the model either overestimates or underestimates the noise level, leading to under-denoising or semantic oversmoothing, respectively. An additional and noteworthy observation is that when t is perturbed within a small margin, such as $\pm 5\%$, the system performance remains relatively stable across all indicators. This demonstrates the robustness of the proposed parameter selection mechanism, suggesting that our framework does not require highly precise

SNR estimation to function effectively. Instead, a coarse approximation of the channel condition is sufficient for achieving near-optimal denoising behavior—an important practical advantage in dynamic or resource-constrained communication scenarios.

Fig. 9 reports similar findings for the scaling factor α . Again, the analytically computed value achieves the best or near-best performance across the board, validating the correctness of our theoretical derivation. The advantage of using the exact value is especially pronounced in low-SNR regimes, such as $\text{SNR} < -2.5\text{dB}$, where even minor inaccuracies in scaling lead to severe mismatches between the input distribution of

Fig. 8: Performance evaluation on different t .Fig. 9: Performance evaluation on different α .

the denoiser and its training distribution. In contrast, the theoretically derived scaling factor enables optimal distribution alignment and preserves denoising fidelity. These results confirm the critical role of precise distribution matching in the success of generative denoising models under severe noise conditions. In summary, the experimental results provide strong numerical evidence supporting the correctness and effectiveness of the closed-form expressions for t and α proposed in Theorems 1 and 2. Moreover, the demonstrated performance robustness to small deviations further highlights the practicality and resilience of our approach in real-world communication systems where estimation errors are inevitable. This validates the proposed framework not only from a theoretical standpoint but also from a system design and deployment perspective.

VI. CONCLUSION

In this work, we have proposed a novel semantic communication framework based on LDMs and have established a rigorous theoretical foundation grounded in stochastic differential equations to guide the denoising process. We have further derived closed-form solutions for the optimal diffusion timestep and input scaling factor, enabling robust semantic reconstruction without requiring model fine-tuning or retraining. By leveraging pretrained generative models and adapting them through analytical mappings to the wireless channel conditions, the proposed method has demonstrated strong generalization, noise resilience, and compatibility with diverse data distributions, making it well-suited for practical deployment in future wireless communication systems. In future work, we will explore the extension of our framework to multi-modal semantic communication tasks, incorporate adaptive diffusion control for real-time applications, and investigate joint

training strategies to further optimize end-to-end performance under dynamic and multi-user network environments.

REFERENCES

- [1] S. Dang, O. Amin, B. Shihada, and M.-S. Alouini, "What should 6G be?" *Nature Electronics*, vol. 3, no. 1, pp. 20–29, 2020.
- [2] P. Zhang, W. Xu, Y. Liu, X. Qin, K. Niu, S. Cui, G. Shi, Z. Qin, X. Xu, F. Wang *et al.*, "Intellicise wireless networks from semantic communications: A survey, research issues, and challenges," *IEEE Communications Surveys & Tutorials*, 2024.
- [3] X. Shen, J. Gao, M. Li, C. Zhou, S. Hu, M. He, and W. Zhuang, "Toward immersive communications in 6G," *Front. Comput. Sci.*, vol. 4, p. 1068478, 2023.
- [4] E. Sisinni, A. Saifullah, S. Han, U. Jennehag, and M. Gidlund, "Industrial internet of things: Challenges, opportunities, and directions," *IEEE transactions on industrial informatics*, vol. 14, no. 11, pp. 4724–4734, 2018.
- [5] N. Cheng, X. Wang, Z. Li, Z. Yin, T. H. Luan, and X. Shen, "Toward enhanced reinforcement learning-based resource management via digital twin: Opportunities, applications, and challenges," *IEEE Network*, vol. 39, no. 1, pp. 189–196, 2025.
- [6] Z. Qin, X. Tao, J. Lu, W. Tong, and G. Y. Li, "Semantic communications: Principles and challenges," *arXiv preprint arXiv:2201.01389*, 2021.
- [7] W. Jiang, B. Han, M. A. Habibi, and H. D. Schotten, "The road towards 6g: A comprehensive survey," *IEEE Open Journal of the Communications Society*, vol. 2, pp. 334–366, 2021.
- [8] D. Gündüz, M. A. Wigger, T.-Y. Tung, P. Zhang, and Y. Xiao, "Joint source–channel coding: Fundamentals and recent progress in practical designs," *Proceedings of the IEEE*, 2024.
- [9] N. Islam and S. Shin, "Deep learning in physical layer: Review on data driven end-to-end communication systems and their enabling semantic applications," *IEEE Open Journal of the Communications Society*, 2024.
- [10] V. N. Vapnik, V. Vapnik *et al.*, *Statistical learning theory*. Wiley New York, 1998.
- [11] I. Goodfellow, Y. Bengio, and A. Courville, *Deep learning*. MIT press, 2016.
- [12] H. Kim, Y. Jiang, R. Rana, S. Kannan, S. Oh, and P. Viswanath, "Communication algorithms via deep learning," *arXiv preprint arXiv:1805.09317*, 2018.
- [13] R. Rombach, A. Blattmann, D. Lorenz, P. Esser, and B. Ommer, "High-resolution image synthesis with latent diffusion models," in *Proceedings of the IEEE/CVF conference on computer vision and pattern recognition (CVPR)*, 2022, pp. 10 684–10 695.

- [14] D. P. Kingma, M. Welling *et al.*, “Auto-encoding variational bayes,” 2013.
- [15] Y. Song, J. Sohl-Dickstein, D. P. Kingma, A. Kumar, S. Ermon, and B. Poole, “Score-based generative modeling through stochastic differential equations,” *arXiv preprint arXiv:2011.13456*, 2020.
- [16] Y. Huang, Z. Qin, X. Liu, and K. Xu, “Simultaneous image-to-zero and zero-to-noise: Diffusion models with analytical image attenuation,” 2024.
- [17] X. Luo, H.-H. Chen, and Q. Guo, “Semantic communications: Overview, open issues, and future research directions,” *IEEE Wireless Communications*, vol. 29, no. 1, pp. 210–219, 2022.
- [18] Z. Lu, R. Li, K. Lu, X. Chen, E. Hossain, Z. Zhao, and H. Zhang, “Semantics-empowered communications: A tutorial-cum-survey,” *IEEE Communications Surveys & Tutorials*, vol. 26, no. 1, pp. 41–79, 2024.
- [19] G. Xin, P. Fan, and K. B. Letaief, “Semantic communication: A survey of its theoretical development,” *Entropy*, vol. 26, no. 2, p. 102, 2024.
- [20] L. X. Nguyen, A. D. Raha, P. S. Aung, D. Niyato, Z. Han, and C. S. Hong, “A contemporary survey on semantic communications: Theory of mind, generative ai, and deep joint source-channel coding,” *arXiv preprint arXiv:2502.16468*, 2025.
- [21] Y. Wang, H. Han, Y. Feng, J. Zheng, and B. Zhang, “Semantic communication empowered 6g networks: Techniques, applications, and challenges,” *IEEE Access*, 2025.
- [22] M. Zhang, M. Abdi, V. R. Dasari, and F. Restuccia, “Semantic edge computing and semantic communications in 6g networks: A unifying survey and research challenges,” *arXiv preprint arXiv:2411.18199*, 2024.
- [23] S. Ye, Q. Wu, P. Fan, and Q. Fan, “A survey on semantic communications in internet of vehicles,” *Entropy*, vol. 27, no. 4, p. 445, 2025.
- [24] S. Ma, B. Shen, C. Zhang, Y. Wu, H. Li, S. Li, G. Shi, and N. Al-Dhahir, “Modeling and performance analysis for semantic communications based on empirical results,” *arXiv preprint arXiv:2504.21055*, 2025.
- [25] A. Creswell, T. White, V. Dumoulin, K. Arulkumaran, B. Sengupta, and A. A. Bharath, “Generative adversarial networks: An overview,” *IEEE signal processing magazine*, vol. 35, no. 1, pp. 53–65, 2018.
- [26] X. Lin, J. He, Z. Chen, Z. Lyu, B. Fei, B. Dai, W. Ouyang, Y. Qiao, and C. Dong, “Diffbir: Towards blind image restoration with generative diffusion prior,” *arXiv preprint arXiv:2308.15070*, 2023.
- [27] J. Austin, D. D. Johnson, J. Ho, D. Tarlow, and R. Van Den Berg, “Structured denoising diffusion models in discrete state-spaces,” *Advances in Neural Information Processing Systems*, vol. 34, pp. 17 981–17 993, 2021.
- [28] J. Ho, A. Jain, and P. Abbeel, “Denoising diffusion probabilistic models,” *Advances in neural information processing systems*, vol. 33, pp. 6840–6851, 2020.
- [29] V. A. Zorich and O. Paniagua, *Mathematical analysis II*. Springer, 2016, vol. 220.
- [30] E. Boursoulatz, D. B. Kurka, and D. Gündüz, “Deep joint source-channel coding for wireless image transmission,” *IEEE Transactions on Cognitive Communications and Networking*, vol. 5, no. 3, pp. 567–579, 2019.
- [31] K. Yang, S. Wang, J. Dai, X. Qin, K. Niu, and P. Zhang, “Swinjscc: Taming swin transformer for deep joint source-channel coding,” *IEEE Transactions on Cognitive Communications and Networking*, 2024.
- [32] T. Karras, T. Aila, S. Laine, and J. Lehtinen, “Progressive growing of gans for improved quality, stability, and variation,” *arXiv preprint arXiv:1710.10196*, 2017.
- [33] J. Deng, W. Dong, R. Socher, L.-J. Li, K. Li, and L. Fei-Fei, “Imagenet: A large-scale hierarchical image database,” in *2009 IEEE conference on computer vision and pattern recognition*. Ieee, 2009, pp. 248–255.
- [34] Z. Wang, A. Bovik, H. Sheikh, and E. Simoncelli, “Image quality assessment: from error visibility to structural similarity,” *IEEE Transactions on Image Processing*, vol. 13, no. 4, pp. 600–612, 2004.
- [35] R. Zhang, P. Isola, A. A. Efros, E. Shechtman, and O. Wang, “The unreasonable effectiveness of deep features as a perceptual metric,” in *Proceedings of the IEEE conference on computer vision and pattern recognition*, 2018, pp. 586–595.